I.P.N. - 91406 ORSAY CEDEX

institut de physique nucléaire CNRS - IN2P3 UNIVERSITÉ PARIS - SUD

IPNO-DRE 00-28

Are narrow mesons, baryons and dibaryons evidence for multiquark states ?

B.Tatischeff and J.Yonnet

Institut de Physique Nucleaire Orsay
F-91406 Orsay Cedex,France

PLEASE BE AWARE THAT
ALL OF THE MISSING PAGES IN THIS DOCUMENT
WERE ORIGINALLY BLANK

IPNO-DRE 00-28

Are narrow mesons, baryons and dibaryons evidence for multiquark states ?

B.Tatischeff and J.Yonnet

Institut de Physique Nucleaire Orsay
F-91406 Orsay Cedex,France

Invited talk at the International Worshop "Relativistic Nuclear Physics: From hundreds MeV to TeV", Stara Lesna, June 26 - July 1, 2000.

Are narrow mesons, baryons and dibaryons evidence for multiquark states ?

B.Tatischeff* and J.Yonnet

Institut de Physique Nucléaire,CNRS/IN2P3, F-91406 Orsay Cedex, France

Several narrow structures have been progressively observed since the last fiften years, in dibaryonic invariant mass spectra or in missing mass spectra. More recently, narrow structures were observed in baryonic and now in mesonic mass spectra. Since these small peaks appear at fixed masses, independently of the experiment, they are associated with real states. There is no room to explain these states within classical nuclear physics taking into account baryonic and mesonic degrees of freedom.

An interpretation is proposed, which associate these narrow structures with two coloured quark clusters.

I. INTRODUCTION

It is usually believed than the observation of quark degrees of freedom cannot start at energies lower than several GeV ($\approx$ 10 GeV). However such limit is somewhat unprecise. A relation was proposed by Baldin [1] some years ago. In this theory, the deconfinement is determined as being a process allowing particle creation for $b_{ij} \geq 5$, where

$$b_{ij} = -(P_i/m_i - P_j/m_j)^2 \quad (1)$$

and P_i, P_j are the four momentum of both particles involved in the reaction, and m_i, m_j their masses. If we consider a N-N reaction, the previous relation reduces in the laboratory system to $T_i \geq 2.35$ GeV.

The search for possible signatures of the beginning of the quark deconfinement, could therefore be significant at energies close to 2 GeV. These will be the energies of the experiments discussed in this paper. This paper will start to describe experimental results, rather than calculations, for the following reasons :

- several accelerators exist (or existed), where the experiments usefull for such studies were already performed and must be repeated,
- calculations must be done using non perturbative QCD. This is a difficult task.

---

*e-mail: tati@ipno.in2p3.fr

The beginning of this work will be dedicated to show the most precise experimental results where narrow hadronic structures were observed. Some of these results were already published, but not all, and the presentation will emphasize recent, unpublished, and sometimes preliminary data. These results were obtained during the study of the $\vec{p}\ p \rightarrow a^+\ b^+\ X$ reaction.

The paper will be divided into the following parts. The experiment will be shortly described. Some spectra will be presented, showing various cheks and studies done in order to control all possible spurious effects. Then several results will be shown, corresponding to narrow dibaryons, narrow baryons and narrow mesons. The third part will describe an attempt to rely these structures to coloured quark clusters. Finally a discussion will be presented, trying to reproduce the masses of **all observed hadronic narrow structures** inside two phenomenological relations and a minimum number (three) of free parameters.

II. EXPERIMENTAL RESULTS

The reaction $\vec{p}\ p \rightarrow a^+\ b^+\ X$ was studied using the SPES3 beam line and detection at SATURNE. The proton beam was accelerated at three energies (T_p=1520, 1805 and 2100 MeV) and the spectrometer put at several angles between 0^0 and 17^0 in the lab. Several papers were already published, describing the experiment [2]. Therefore a general description will not be repeated here. However since the objective of these experiments is to look for small peaks lying over a background, spacial care on possible experimental errors must be done. Some of these checks are described now.

A. Misidentified particles

The electronical device included two time of flights. The first one, on a 3 meter basis, identified the particles. The second one between both detected particles, controled the random events, and rejected the small amount of misidentified particles. Indeed, the distance inside the spectrometer, from target up to detection, of the order of 7 meters, induced a shift $\approx$ 21 channels (of 250 ps/channel), if the nature of the detected particle was changed from proton to pion. This is much larger than the window used to keep two particle real events ($\pm$ 9 channels). Only some **random** coincidences between a real proton and a misidentified pion - when a p p $\rightarrow$ p p X reaction was studied - were not suppressed by our electronical selection. There were very few such events, without any peak, as shown in Fig. 1.

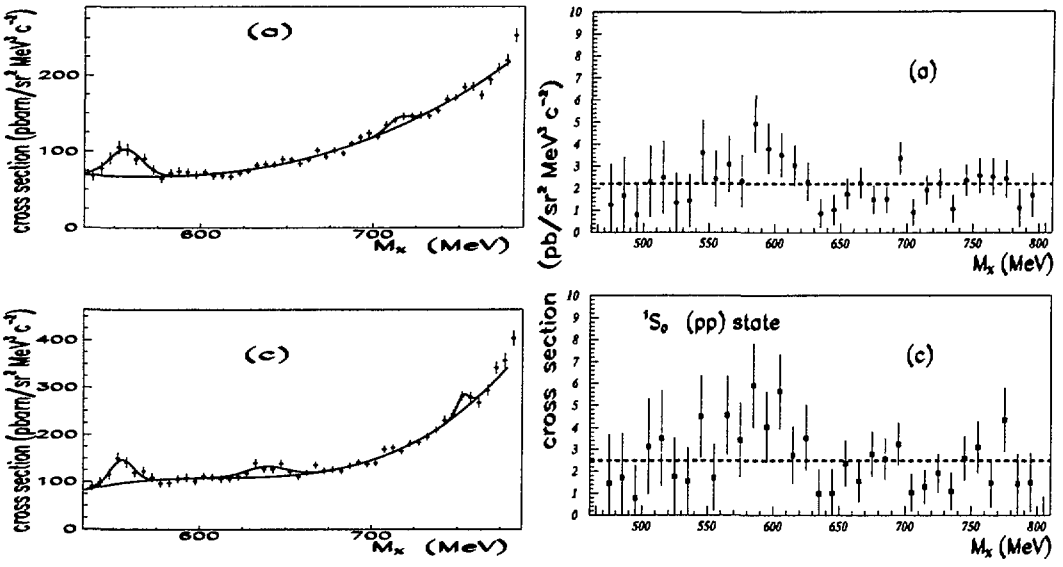

Fig. 1. Cross sections versus the missing mass M_X of the p p $\rightarrow$ p p X reaction at T_p=2.1 GeV, θ=9^0 lab. Real events on left part of the figure and misidentified events on right part. The two cases (a) and (c) correspond to different conditions on the invariant mass M_{pp} of both detected protons.

B. Range of scatterplot selection

The scatterplot of the momenta of the first detected particles against the momenta of the second detected particles, displayed sharp angles (Fig. 2). These were due to cuts induced by physics and by the spectrometer momenta limits. They were also lost events, induced mainly by those events when both momenta were equal. This explains the empty narrow region inside the filled area in top of Fig. 2. A simulation code was written in order to correct all lost events. However when the correction fonction displayed peaks, the measured range was limitated in order to eliminate such regions and to avoid to introduce eventual fake effects (see Fig. 2).

C. Empty target contribution

Fig. 3 shows the missing mass spectra M_X of the p p $\rightarrow$ p π^+ X reaction, after removal of all events corresponding to n and Δ^0 missing masses, in order to enhance the intermediate region corresponding to narrow baryons. The empty target data, normalized on the same number of incident protons, are shown at the bottom of the figure. We observe here a low count rate ($\leq$ 5 %) and a flat distribution without

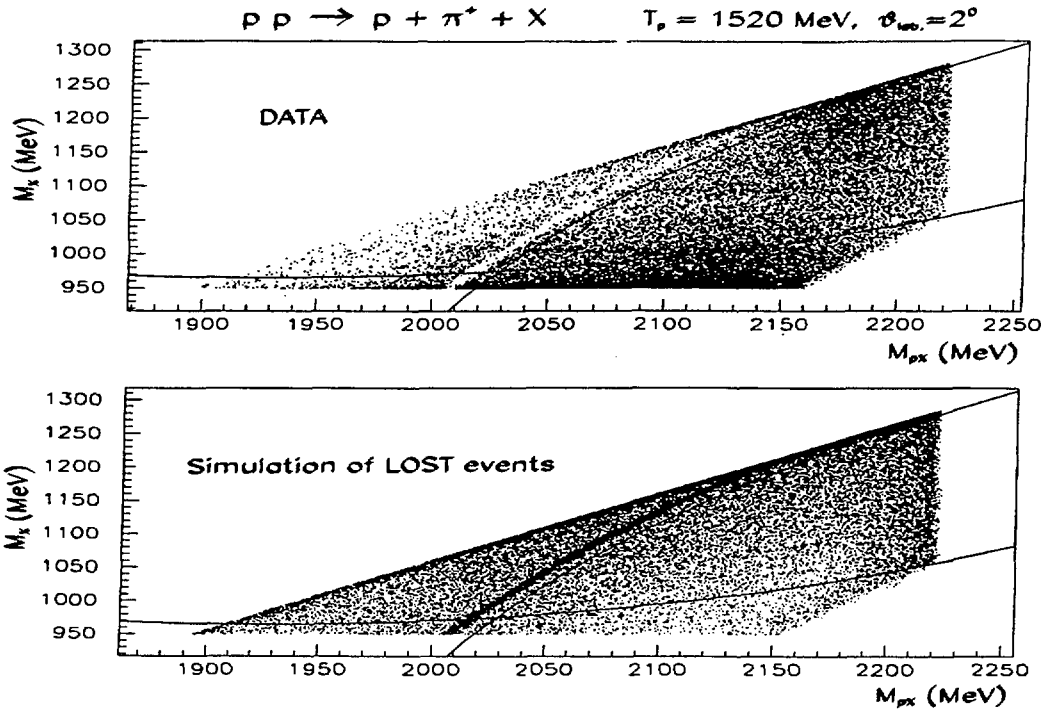

Fig. 2. Scatterplot of the missing mass M_X versus the invariant mass M_{pX} events for the pp→pπ^+X reaction at T_p= 1520 MeV and θ=2^0. The area between both curves was selected, at the expense of statistics, in order to avoid sharp corrections. The intense region corresponding to n missing mass peak was removed in these data.

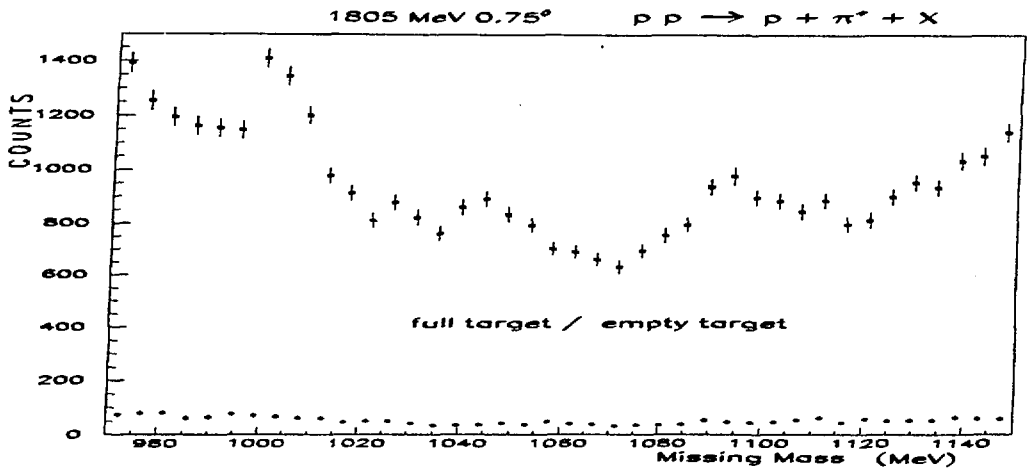

Fig. 3 Comparison of full versus empty target countings.

any structure. We deduce from this observation that our data were not spoiled by a beam tail scattering inside some thick side of the cryogenic target or the scattering chamber.

D. Random events

The incident proton flux was adjusted in order to keep, during the acquisition, the number of random events at a rate lower than 10 %. Then the contamination of randoms, in the window of real events, was small for p p → p π^+X and p p → p p X reactions. Fig.4 shows the small and smooth distribution of these events for p p → p π^+ X reaction. The number of true events in case of p p → $\pi^+\pi^+$ X reaction was small, and therefore the amount of random events was large. For this last reaction, the results corresponding to random events only, will also be shown for comparison.

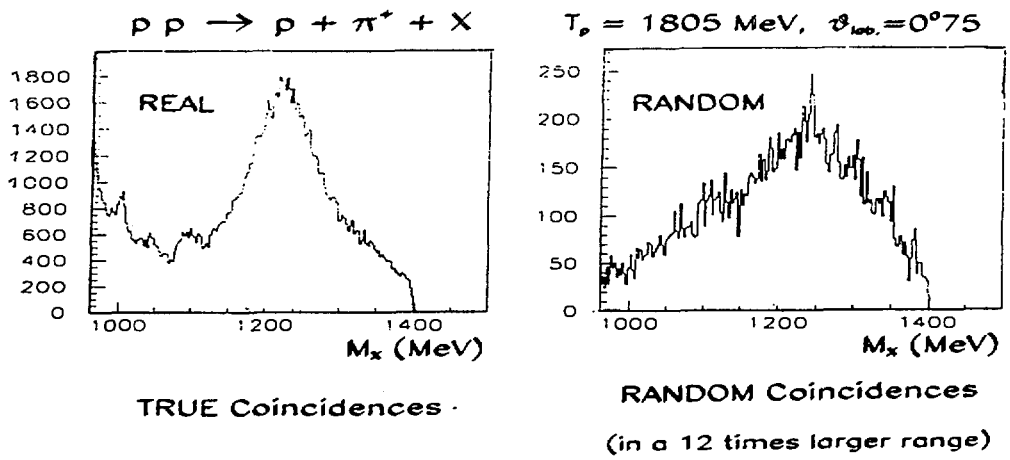

Fig. 4 Comparison of real with random events.

III. RESULTS

Three reactions were studied simultaneously. They were :

1) **p p → p π^+ X**. Here the baryonic missing mass M_X was studied in the range $940 \leq M_X \leq 1470$ MeV. All ranges depended on the incident energy and angle of measurement. In the same reaction, the dibaryonic invariant mass M_{pX} was studied in the range $1950 \leq M_{pX} \leq 2400$ MeV.

2) **p p → p p X**. Here the mesonic missing mass M_X was studied in the range $135 \leq M_X \leq 800$ MeV. The dibaryonic invariant mass M_{pp} was studied in the range $1877 \leq M_{pp} \leq 1920$ MeV.

3) **p p → $\pi^+\pi^+$ X**. Here the dibaryonic missing mass M_X was studied in the range $1880 \leq M_X \leq 2138$ MeV.

The results will be presented now, using a classification by hadronic species and not by reactions.

A. Narrow dibaryons

The observation of narrow structures, which correspond to non classical physics, started more than 15 years ago in the dibaryonic sector. A classification of the observed masses was reported 10 years ago in a review talk [3]. These first results were progressively confirmed. Recently new precise data were published [2] which correspond to the reaction p p→p π^+ X from the experiment described before. A selection of typical spectra are shown in Fig. 5, 6 and 7 where the dibaryons were observed in M_{pn} and

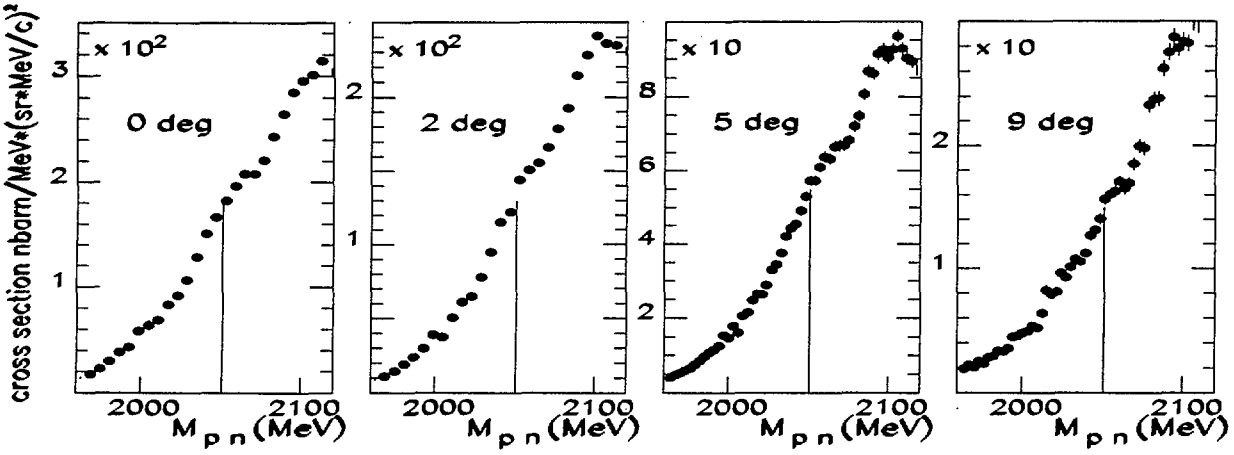

Fig. 5. p p → p π^+ n reaction at T_p = 1520 MeV, showing a narrow dibaryon at 2050 MeV.

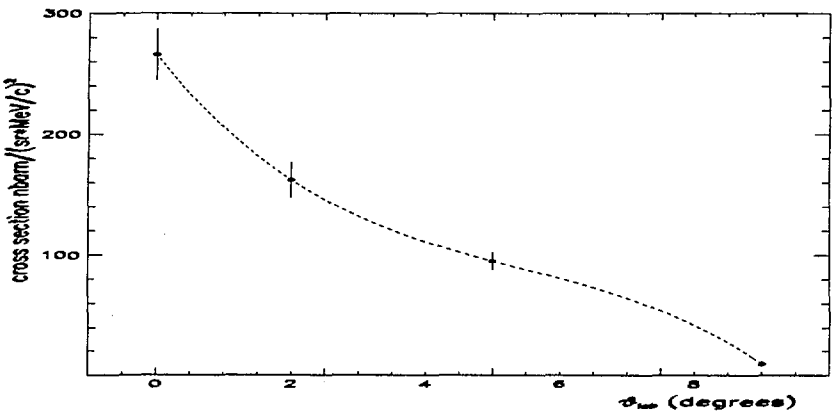

Fig. 6. Forward angle angular distribution of the M = 2050 MeV dibaryon produced in the p p → p π^+ n reaction at T_p = 1520 MeV.

M_{pX} invariant masses in reaction 1). Narrow dibaryons were observed in the invariant mass spectra at 2050, 2122 and 2150 MeV. The corresponding numbers of standard deviations vary between 3.2 and 12.6.

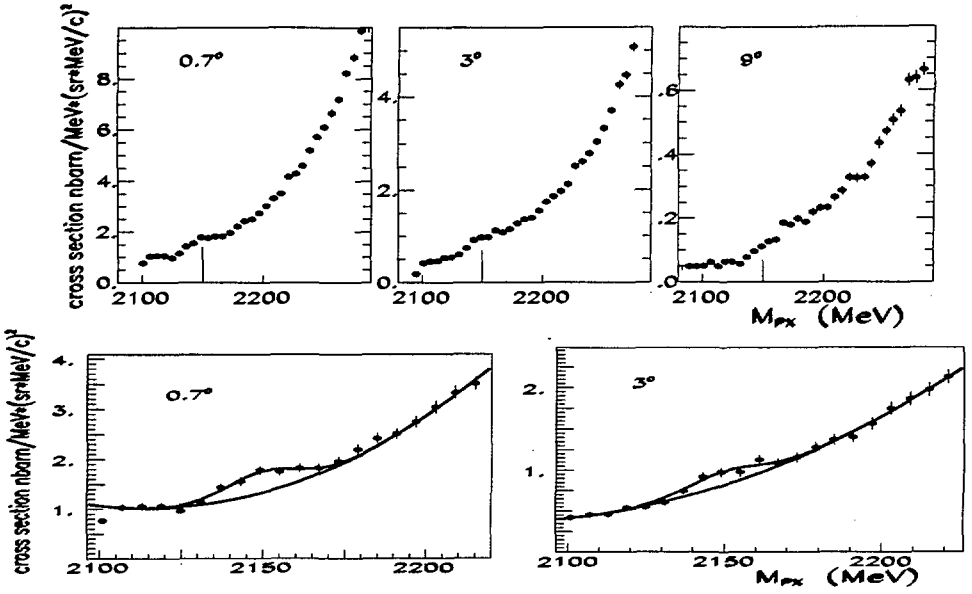

Fig. 7. p p → p π^+ X reaction at T_p = 2100 MeV, showing a narrow dibaryon at 2150 MeV. The number of standard deviations (S.D.) at $\theta_{lab.} = 0.7^0$ (3^0) is equal to 8.1 (5.5).

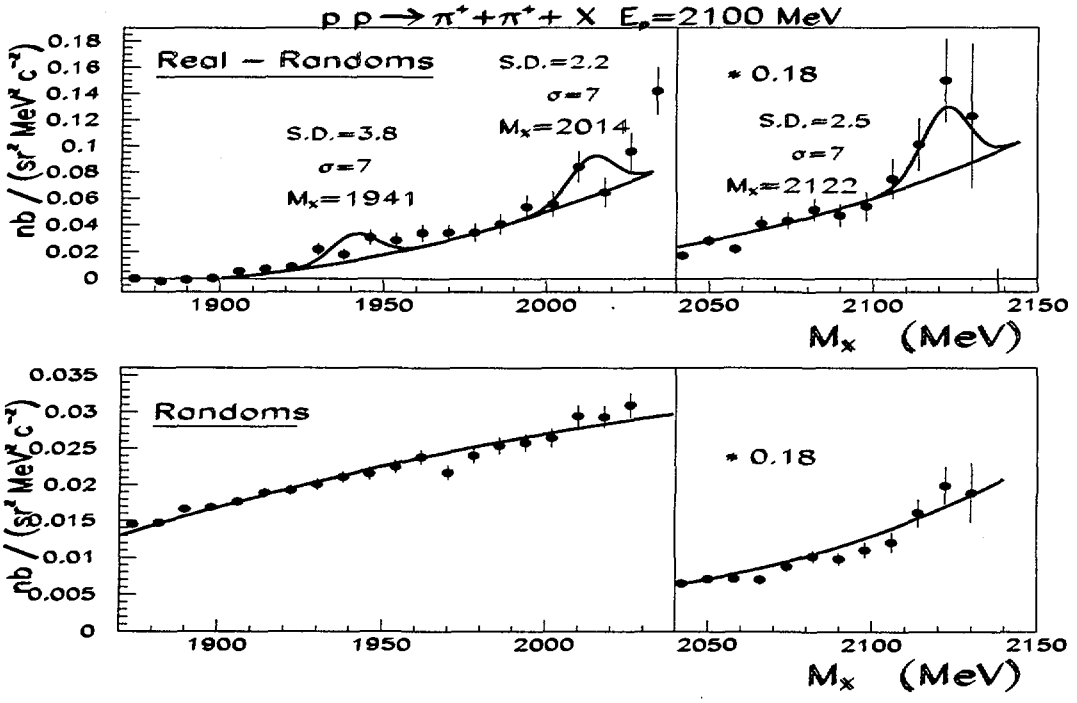

Fig. 8. p p → π^+ π^+ X reaction at T_p = 2100 MeV. Narrow dibaryons at 1941, 2014 and 2122 MeV are observed in the real minus random events spectrum (sum of all three angles measured at this energy). The random spectrum, normalized on the same coincidence window width, is more precise and does not

display any structure.

The masses of these narrow dibaryons agree with systematic studies of dibaryonic masses experimentally observed through many experiments performed by varius collaborations.

The p p $\rightarrow$ π^+ π^+ X reaction was only analyzed at T_p = 2100 MeV, since the number of two pion produced events, already low at this energy, is still less at smaller energies. Preliminary results are shown in Fig. 8. We observe that the results of this new reaction, are rather imprecise. They are however in agreement with the previous results. Indeed the three dibaryon masses observed at 1941, 2014 and 2122 MeV were already obtained previously in several different experiments [3].

The actual classification of narrow dibaryons, including the presently shown results are displayed in Fig. 9 and summarized in Fig. 10. Here the experiments performed with electronics are noted with squares, and those from bubble chamber chambers are noted with triangles. Full symbols correspond to data with S.D. $\geq$ 3.07 (confidence level $\geq$ 99%), and open symbols to data with S.D. $\leq$ 3.07.

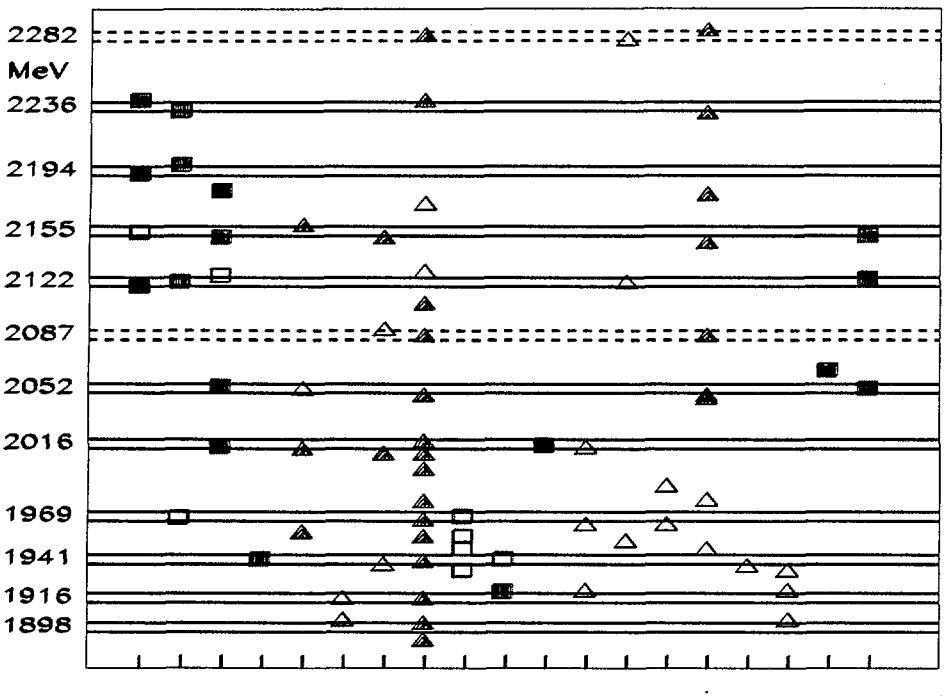

Fig. 9. Masses of experimental narrow dibaryons observed in previous and present experiments, versus the corresponding reference quoted in [2].

Fig. 9 shows that two regions can be roughly observed. In the first region : 2 GeV $\leq$ M_{pp}, nearly all dibaryonic experimental masses fall into narrow bands which correspond to a well fixed mass $\pm$ 3 MeV. In the second region, for masses lower than 2 GeV, the situation is somewhat confused. The threshold for ppπ desintegration is 2.016 GeV.

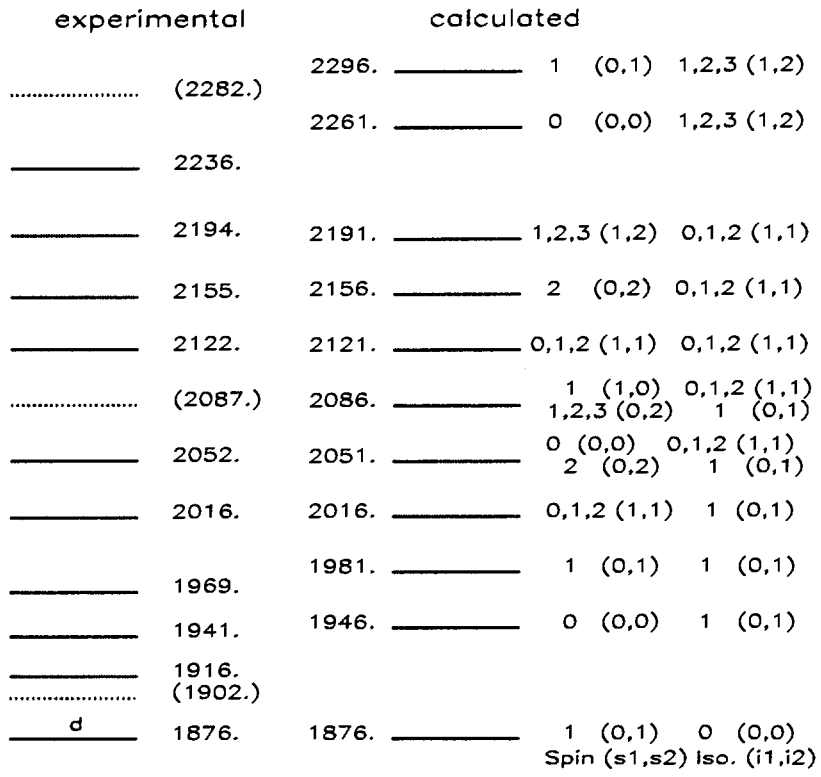

Fig. 10. Experimental spectra of narrow dibaryons and calculated masses, before precise study of the region $2M_p \leq M_{pp} \leq 2.0$ GeV. The calculations will be discussed later.

We need a precise experiment dedicated to this mass region. This was done by the study of the invariant M_{pp} mass spectra through the reaction 2) : p p $\rightarrow$ p p X. A selection of typical spectra from such reaction is presented in Fig. 11. These data are preliminary. The cross sections do show small peaks or shoulders. Since all statistics was concentrated in a relatively narrow range, it was possible to extract structures with a large S.D. although in this mass range, the dibaryon production cross sections are small. Since the electromagnetic disintegration only is allowed, the widths of the observed structures are experimental. Due to the fast decrease of the counting for increasing M_{pp}, the statistical precision in that experiment was too small for masses larger than 1920 MeV.

As it was the case in all reactions described, the analyzing powers were measured simultaneously with the cross-sections. Although the corresponding error bars are larger than those obtained for cross sections, their shape in several cases display an oscillatory pattern shown in Fig. 12. These oscillations **may be** the consequence of an interference between the classical NN amplitude and another amplitude, quickly varying for different M_{pp} invariant masses. The existence of several narrow dibaryons in this mass range **could be** at the origin of such behaviour.

Fig. 13 shows the spectrum of low mass dibaryons obtained from this experiment, and compared with

previously observed low mass dibaryons.

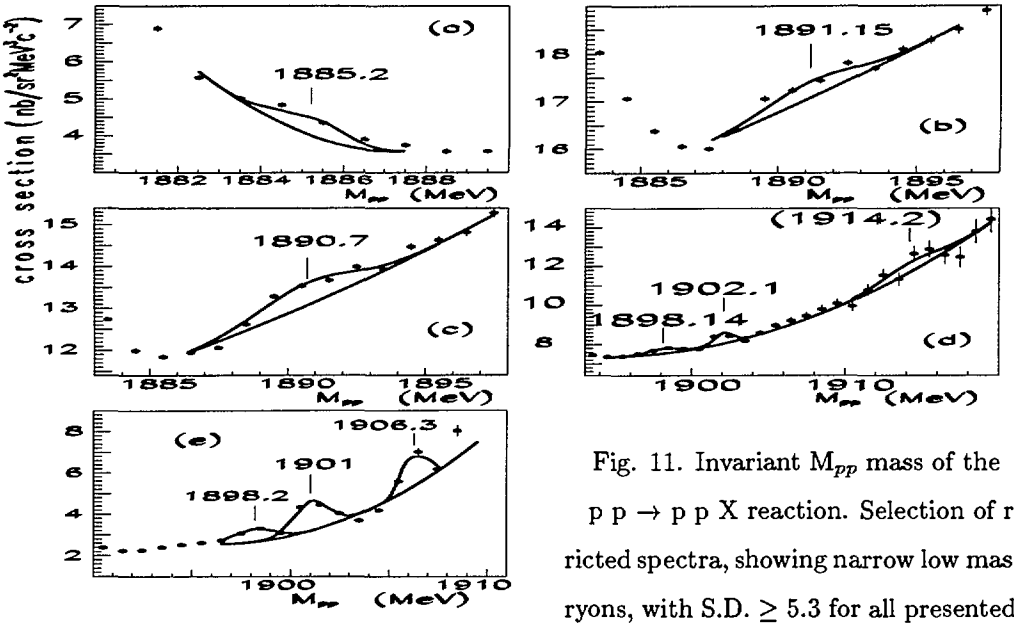

Fig. 11. Invariant M_{pp} mass of the p p $\rightarrow$ p p X reaction. Selection of restricted spectra, showing narrow low mass dibaryons, with S.D. $\geq$ 5.3 for all presented peaks (except those close to 1915 MeV, and the 1902.1 structure in part (d)). The five parts of the figure correspond to : (a) T_p=1520 MeV; (b) all energies and angles; (c) T_p=1520 and 1805 MeV; (d) T_p=1520 MeV and forward c.m. data at T_p=1805 MeV; (e) T_p=1805 MeV, backward c.m. data at 0.75^0 and 3.7^0.

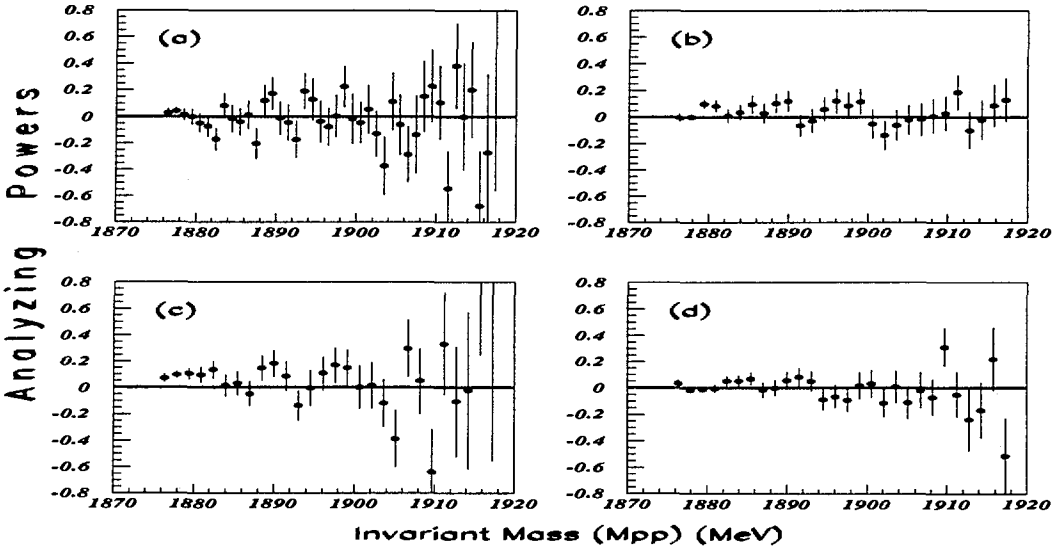

Fig. 12. Analyzing powers for the $\vec{p}$ p $\rightarrow$ p p X reaction, at T_p=1805 MeV: (a) and (c), and at T_p=2100 MeV: (b) and (d). (a) and (b) are for 0.75^0lab. (backward solution in c.m.), (c) for 6.7^0lab. (also backward) and (d) for 9^0lab. forward solution in c.m. system.

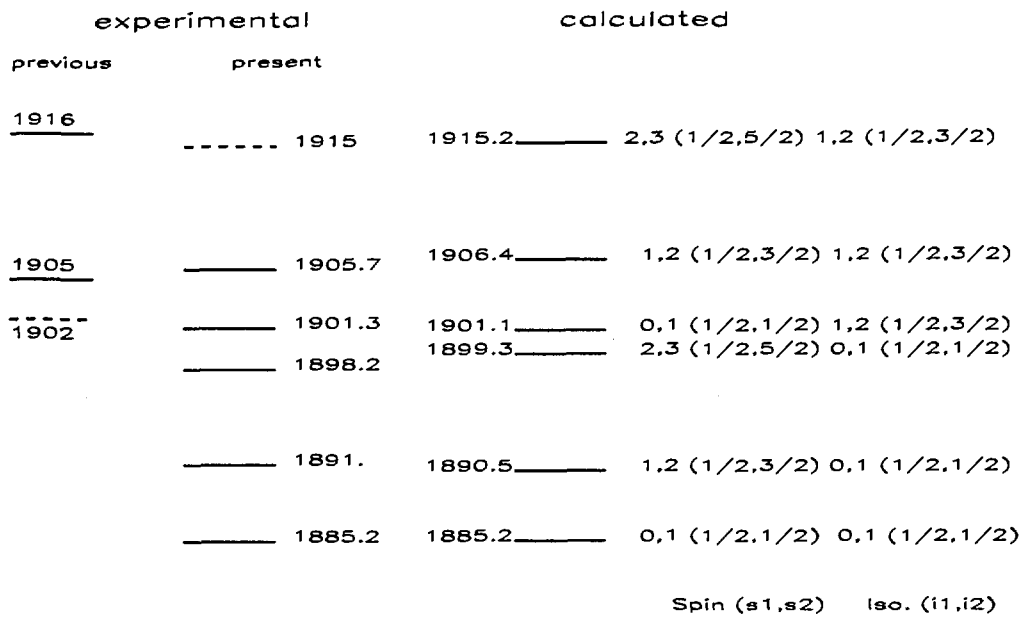

Fig. 13. Masses of low mass dibaryon spectrum, experimental and calculated (mean values from different data). The calculations will be discussed later. The previous masses correspond to references : [5], [6], [7].

B. Narrow Baryons

Narrow exotic baryons at M_X = 1004, 1044 and 1094 GeV, were observed in the missing mass of the p p $\rightarrow$ p π^+ X reaction [4]. Fig. 14 shows a selection of spectra at both smaller energies and forward angles. Filled data are for T_p = 1805 MeV and empty data are for T_p = 1520 MeV. We observe that the structures appear at constant missing masses : 1004, 1044 and 1094 MeV. Fig. 15 shows the new baryonic specta in the range $M_N \leq M_X \leq M_{Roper}$.

C. Narrow Mesonic Structures

They were studied in the missing mass of the p p $\rightarrow$ p p X reaction. The range was cut into two parts : a first part, in the ABC region (below the η meson (550 MeV)), deserves a special discussion since several peaks are not separated. This discussion will be presented elsewhere [9]. We present here the results [10] corresonding to the range 550 MeV (η meson)$\leq M_X \leq$ 783 MeV (ω meson). A selection of typical spectra is shown in Fig. 16 at T_p=1.805 GeV and Fig. 17 at T_p=2.1 GeV.

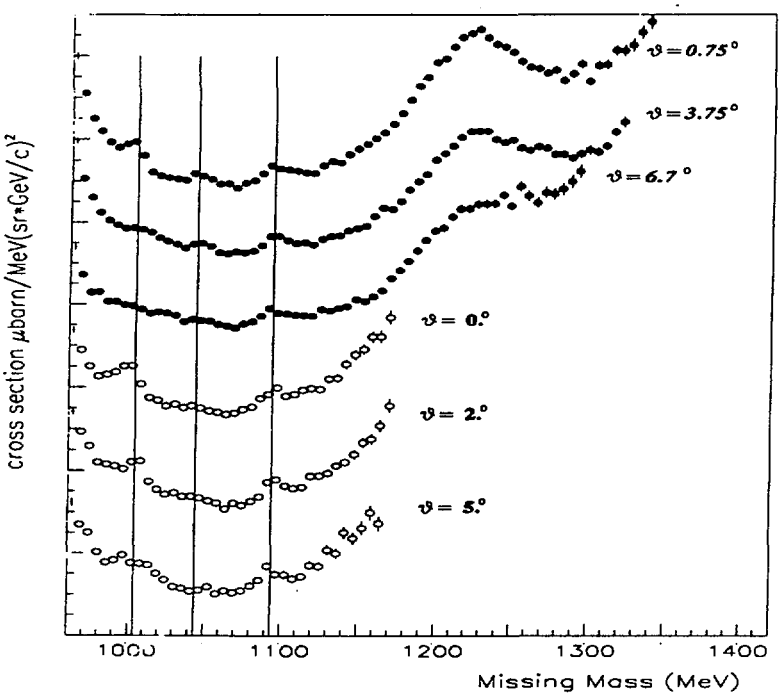

Fig. 14.

Cross sections of the p p → p p X reaction, at forward angles, after cuts on the neutron missing mass. We observe peaks at fixed masses, indicated by vertical lines.

Filled data are for $T_p = 1800$ MeV and empty data are for $T_p = 1520$ MeV.

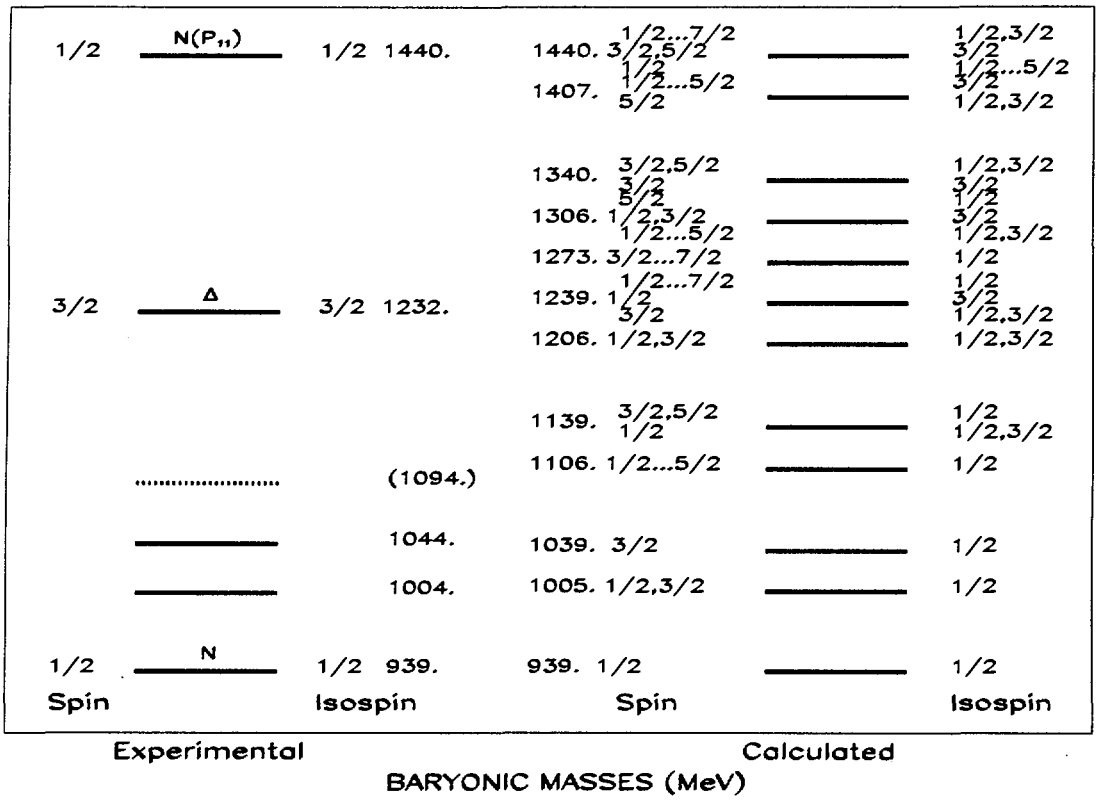

Fig. 15. Baryonic level scheme. The calculated values will be discussed later.

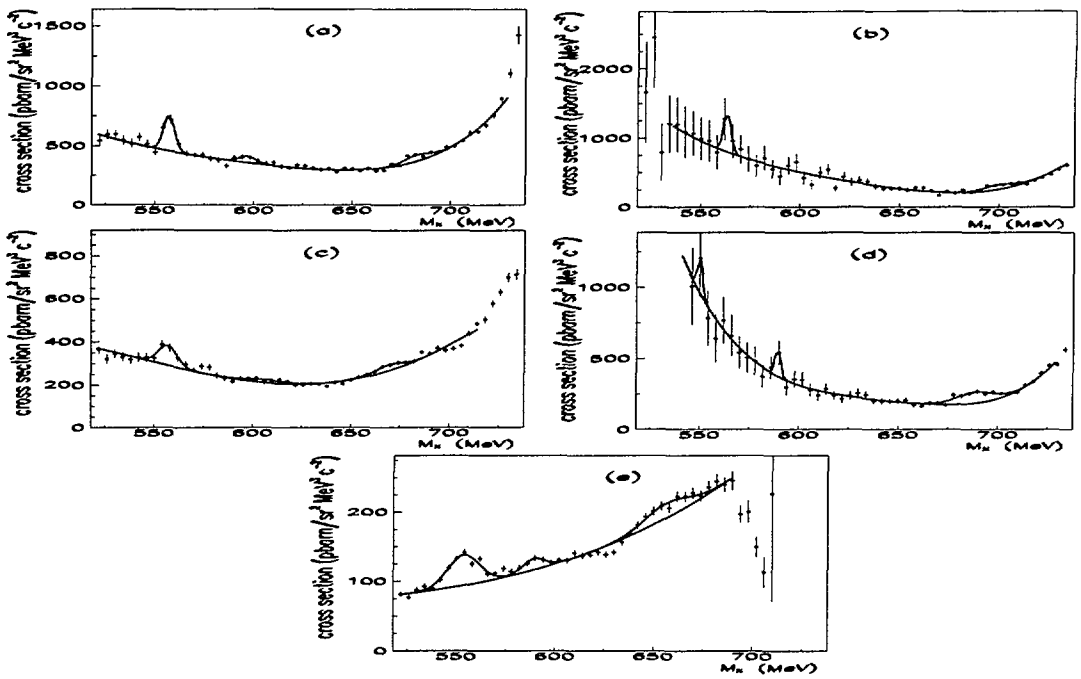

Fig. 16. Differential cross sections (in lab. system) at T_p = 1805 MeV. (a) and (b) correspond to 0° lab. data, (c) and (d) correspond to 3° lab. data and (e) corresponds to 9° lab. data. (a), (c) and (e) correspond to forward kinematics whereas (b) and (d) correspond to backward kinematics.

The spectrum of narrow exotic mesons (between 550 and 800 MeV) is shown in Fig. 18. The left column shows our results which are compared to other data (next column). Narrow mesons were looked for previously in the invariant masse $M_{\pi^+\pi^-}$ ($M_{\pi^-\pi^-}$) [13] from the reaction p n $\rightarrow$ p p π^+ π^- π^- π^0 (p n $\rightarrow$ n p π^+ π^+ π^- π^-) at Dubna using a 5.10 GeV/c neutron beam. Here the statistics was not rich since bubble chamber slides were analyzed. Another experiment was performed at Protvino with 40 GeV π^- beam. Invariant masses $M_{\pi^+\pi^-}$ from the π^- C $\rightarrow$ π^- π^- π^+ C reaction were studied. Several structures were not pointed out by the authors, since they exhibit a too small number of S.D. However their masses are rather close to ours. The masses (in MeV) of these structures compared to our masses between parenthesis, are : 355(350), 440(430), 510, 588(588), 640(647) and 753(750). Although these structures cannot be used by themselves (small S.D.), they however confirm our results.

IV. INTERPRETATION

A. General Description

An interpretation is suggested within the assumption of two coloured constituent quark clusters.

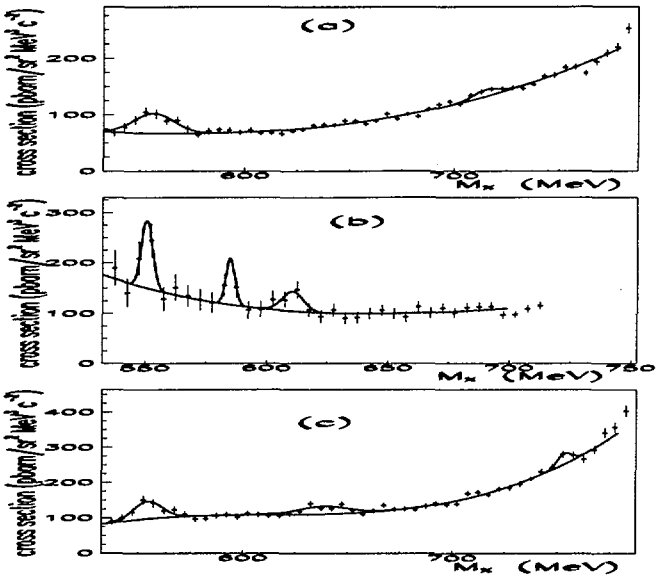

Fig. 17. Differential cross sections (in lab. system) at $T_p = 2100$ MeV, $\theta = 9^o$ lab. (a), (b) and (c) correspond respectively to: forward c.m. kinematics, backward c.m. kinematics and selected $2M_p \leq M_{pp} \leq 2M_p + 5$ MeV events with forward c.m. kinematics.

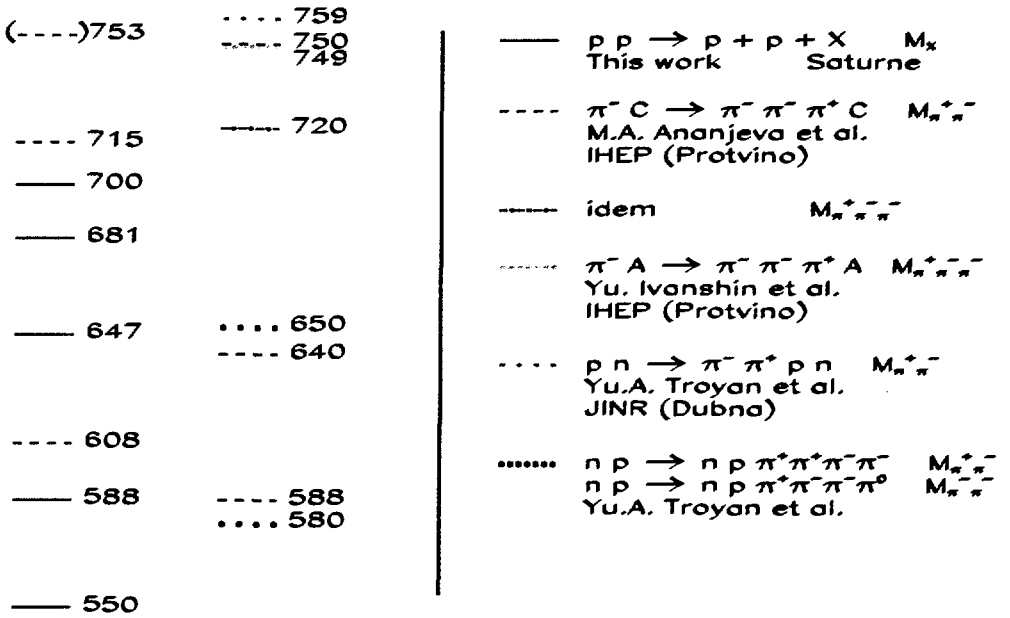

Fig. 18. Masses of narrow exotic mesons. The left column shows the results of this work, when next to the right column shows masses from other experiments [11], [12], [13].

The mass formula used - which involves a large degeneracy - was derived many years ago [14]:

$$M_{\,exp} = M_{0\,exp} + M_{1\,exp}\,[i_1(i_1+1) + i_2(i_2+1) + (1/3)s_1(s_1+1) + (1/3)s_2(s_2+1)] \qquad (2)$$

where i_1 (i_2) and s_1 (s_2) are the isospin and spin values of the first (second) quark cluster. We have two sets of quarks in a bag stretched for orbital excitations. All quarks are in the lowest bag mode (1s ground state of a spherical bag). There is no orbital, neither radial excitation. The spectra is given by the color-magnetic energy. The fine structure is determined by the coloured quark configurations at the ends of the bag.

The experimental results were fitted using the previous formula as a phenomenological one. Both parameters $M_{0\,exp.}$ and $M_{1\,exp}$ were adjusted to the data. Depending on the hadrons considered, these parameters will be adjusted in order to get known mass, spin and isospin of some stable hadrons. Therefore we have either two, one or zero free parameters.

B. Results

For **narrow exotic mesons** we do the assumption that the simplest (lowest) configurations are favoured. We have two free parameters and the following clusters :

$q^2 - \bar{q}^2$ clusters with $M_{0\,exp.} = 310$ MeV, and $M_{1\,exp.} = 30$ MeV describe the ABC mass region (not discussed here), up to M = 470 MeV.

$q^3 - \bar{q}^3$ clusters with the same values of both parameters, describe the mesonic mass range up to 610 MeV.

$q^4 - \bar{q}^4$ clusters. $M_{0\,exp.} = 357$ MeV, and $M_{1\,exp.} = 27$ MeV describe the mesonic mass range up to 790 MeV. The comparison between these calculated masses and those observed experimentally, is shown in Fig. 19.

The parameters for **narrow exotic baryons** are adjusted in order to get the N and N^* (1440) (Roper Resonance) masses, spins and isospins. There is no free parameter here. We get : $M_{0\,exp.} = 838.2$ MeV, and $M_{1\,exp.} = 100.3$ MeV. The calculated mass values are compared to the experimental ones in Fig. 15. The possible spin and isospin values are shown. The parity depends on the clusters : P = + for $[q - q^2]$ clusters, P = - for $[(q\bar{q}) - q^3]$ clusters and P = + for $[(q\bar{q})^2 - q^3]$ clusters. The masses of the two first (3/2, 3/2) states are found to be close to 1232 MeV, a little below and a little above the mass of the known Δ^{++} resonance.

Two sets of clusters are considered for **narrow exotic dibaryons**. The mass region between 1940 and 2300 MeV is described by $q^2 - q^4$ clusters, with $M_{0\,exp.} = 1841$ MeV and $M_{1\,exp.} = 52.5$ MeV.

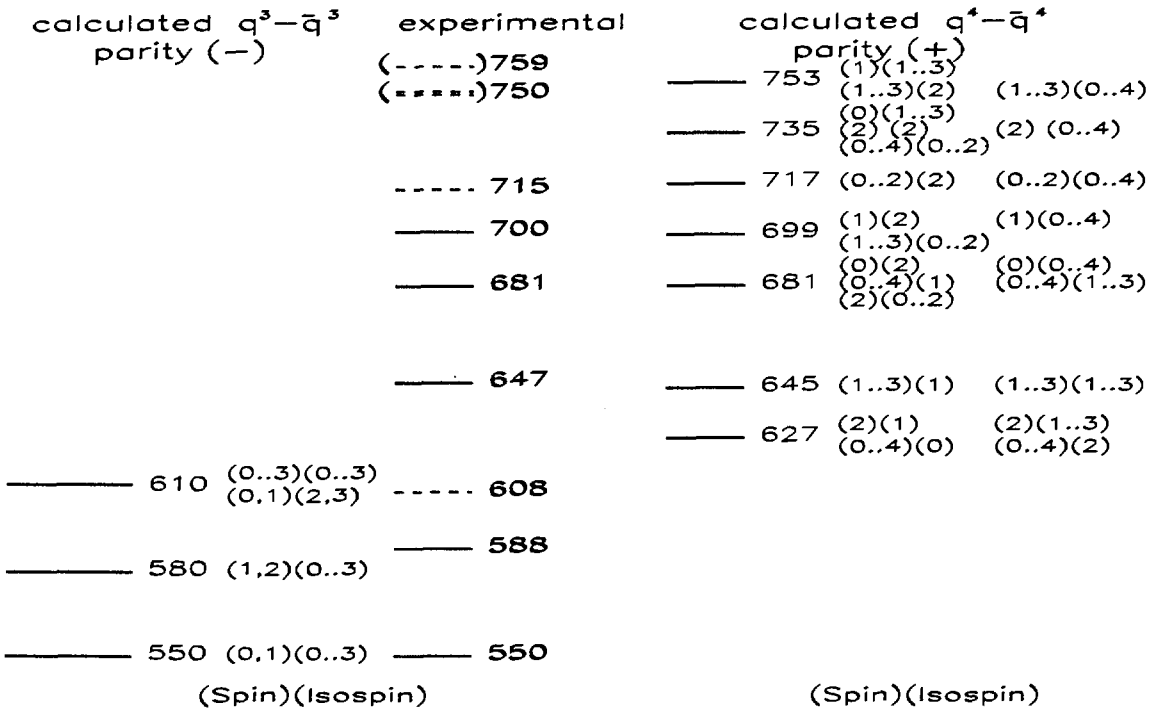

Fig. 19. Experimental and calculated mesonic mass spectrum.

Since these values allow to get deuteron mass, spin and isospin values, only one parameter is free. Fig. 10 shows the comparison between the experimental and calculated masses. We notice here the very good agreement between both, in the mass range $2.0 \leq M \leq 2.2$ GeV.

The mass region between the threshold and 1920 MeV is described by $q - q^5$ clusters, with two free parameters : $M_{0\ exp.} = 1874.6$ MeV and $M_{1\ exp.} = 5.3$ MeV. The comparison is shown in Fig. 13.

C. Attempt for an unification

In order to strengthen our results, we tried to connect the different $M_{0\ exp.}$ and $M_{1\ exp.}$ found for the various following quark clusters :

$$q - q^2,\ q(q\bar{q})^2 \text{ - } q^2,\ q^2 \text{ - } q^4,\ q - q^5,\ q^2 \text{ - } \bar{q}^2,\ q^3 \text{ - } \bar{q}^3 \text{ and } q^4 \text{ - } \bar{q}^4.$$

In order to get a completely general formula for M_0 and M_1, we consider the following two quark clusters :

$$q^m\bar{q}^{\bar{m}} - q^n\bar{q}^{\bar{n}} \qquad (3)$$

where m ($\bar{m}$) and n ($\bar{n}$) are respectively the number of quarks (antiquarks) of both clusters. Let us define the two following variables :

$$u = |(m - \bar{m}) - (n - \bar{n})| \tag{4}$$

and

$$v = |(m - \bar{m}) + (n - \bar{n})| \tag{5}$$

describing the difference and the sum of the number of quarks (minus antiquarks) of both clusters. We calculate $M_{0\ cal.}$ and $M_{1\ cal.}$ using the following expressions :

$$M_{0\ cal.} = M_{00} + M_{01}/v^{v} - M_{1\ cal.} \tag{6}$$

and

$$M_{1\ cal.} = M_{10} + M_{11}/u^{u} \tag{7}$$

where $M_{00} = v.m_q$, m_q313 MeV being the mass of the constituent quarks. We choose $M_{01} = 340$ MeV, $M_{10} = 30$ MeV and $M_{11} = 70.5$ MeV in order to fit the parameters for q^3 - $\bar{q}^3$ clusters. Then the calculated $M_{0\ cal.}$ and $M_{1\ cal.}$ values are compared, for all quark cluster combinations, to the corresponding experimentally determined values in table 1 and Fig. 20.

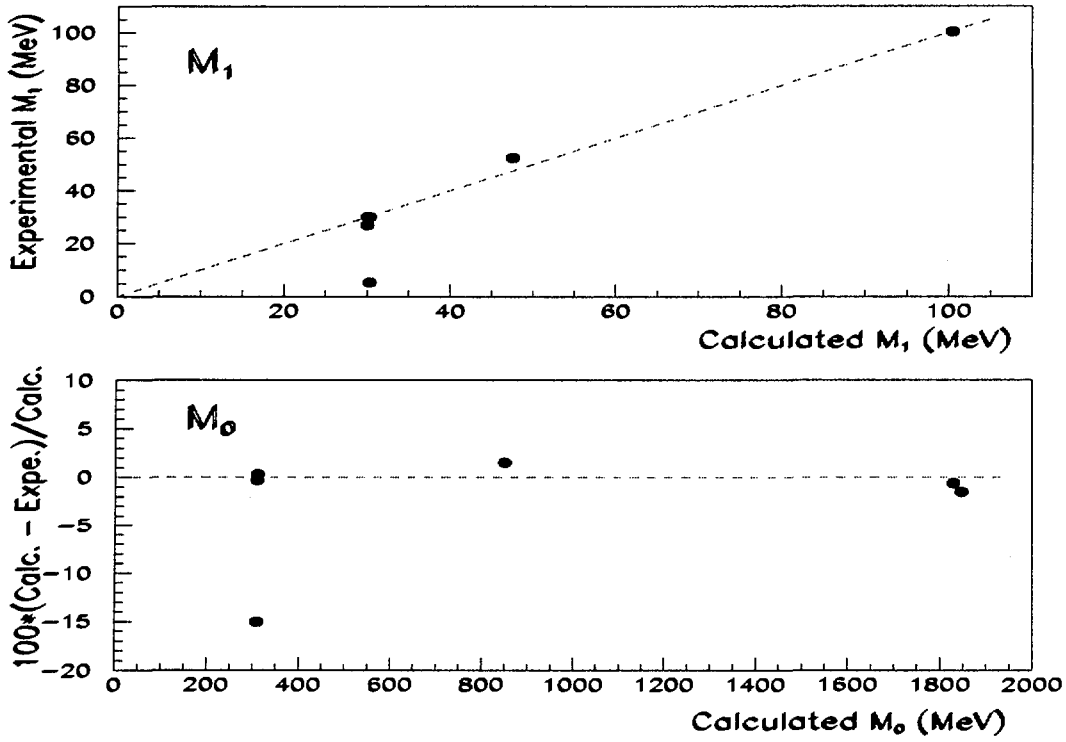

Fig. 20. Comparison of experimentally found M_0 and M_1 values with the corresponding ones obtained from previous equations.

Therefore three adjustable parameters : M_{01}, M_{10} and M_{11} - and the previous formula, allow to reproduce nearly all values reported in table 1. The only parameter which is badly reproduced is the smaller one, M_1 for $q-q^5$ clusters. We observe that the narrow structure masses remain the same when $(q\bar{q})^k$ configurations are added in one or both clusters, (k) being an arbitrarily integer. This appears in $q(q\bar{q})^2$ - q^2 configuration which gives the same mass as the $q-q^2$ configuration.

The formula and parameters give also with high precision the masses of all nuclei. For example the three nucleon mass is obtained within $\Delta M = (M_{cal.} - M_{exp.})/ M_{exp.} \leq 0.003$. On the other hand, the pion mass is badly reproduced (387.6 MeV). In conclusion with the use of our mass formulas and three free parameters, we reproduce the masses of many narrow mesons, baryons and dibaryon experimentally observed.

V. CONCLUSION

The evidence concerning the real existence of narrow hadronic structures, once uncertain, is now clearly established. Indeed the number of standard deviations for narrow peaks against background, vary up to 4.6 for mesons, up to 16.9 for baryons and up to 8.1 for dibaryons. The stability of the corresponding masses, independently of the experiments, allows us to consider them as being new exotic states, which have no room in classical meson-baryon physics. Therefore this work can be considered as an attempt to go beyond the physics of mesons and baryons in interaction.

After having presented the last and more precised experimental results, we have shown the possibility to rely these observations to possible colored quark clusters. In such case, these states will be associated to possible partial precursor quark deconfinement.

It is clear that more work is needed.

Theoretically it corresponds to an important and difficult field, since the energy is low, and therefore involves non-perturbative QCD calculations.

New experiments are essential. They must be precise, with small both systematical and statistical errors. A necessary good resolution ($\sigma \approx$ 1-2 MeV) is more easy to be obtained with not too large energy beams. An incident energy of T $\approx$ several GeV, is well suited for such purpose. These structures must be looked for in inelastic channels. It is not the place here to give an exhaustive list of possible experiments. Some studies were already performed but must be repeated with better accuracy, using the Nuclotron,COSY,CELSIUS... beams. They correspond to the following experiments :

- Isospin zero narrow dibaryons :

  d d $\rightarrow$ d X reactions (Saturne) [15]

- Isospin two narrow dibaryons :

  d $(\pi^{\pm}, \pi^{\mp})$ X (Lampf) [16]

  $\vec{p}\,p \rightarrow \pi^{-}$ X (Saturne) [17]

  stopped π^{-} in D_2 (Triumf) [18]

- Isospin three narrow dibaryons :

  $\vec{p}\,p \rightarrow \pi^{-}\,\pi^{-}$ X (Saturne) [19]

In the same way, the electromagnetic probe can be used for such studies, at TJNAF for exemple. Precise and simple reactions as p [d] (e,e') X must be done in order to look for narrow structures in the missing mass. Of course, many experiments with nucleons and pions in the final state, can be used to the same studies in the invariant masses.

---

[1] A.M. Baldin, Dubna 1992 JINR preprint, E1-92-487.

[2] B. Tatischeff *et al.*, Phys. Rev. **C59** (1999) 1878.

[3] B. Tatischeff *et al.*, Proceedings of the Xth International Seminar on High Energy Physics Problems, Dubna 1990, World Scientific editor, p 177; *ibid* Proceedings of the XII International Seminar on High Energy Physics Problems, Dubna 1994, p62.

[4] B. Tatischeff *et al.*, Phys. Rev. Lett. **79** (1997) 601.

[5] L.V. Fil'kov *et al.*, Phys. Rev. **C61**, 044004 (2000).

[6] V.B. Ganenko *et al.*, JETP Letters **50** (1989) 224.

[7] Yu.A. Troyan and V.N. Pechenov, Sov. J. Nucl. Phys. **56** (1993) 191, in russian.

[8] N. Angelov *et al.*, JINR preprint, P1-88-905.

[9] J. Yonnet *et al.*, submitted to Phys. Rev. C.

[10] B. Tatischeff *et al.*, Phys. Rev. **C62**, 054001 (2000).

[11] M.A. Ananjeva *et al.* JINR P1-98-378, in russian.

[12] Yu. Ivanshin *et al.*, IL NUOVO CIMENTO **107A** (1994) 2855.

[13] Yu.A. Troyan *et al.*, JINR Rapid Communications 5[91]-98, p 33; Proceedings of the Xth International Seminar on High Energy Physics Problems, Dubna 1990, World Scientific editor, p 149.

[14] P.J. Mulders, A.T. Aerts and J.J. de Swart, Phys. Rev. **D21** (1980) 2653; Phys. Rev. **D19** (1979) 2635; Phys. Rev. Lett. **40** (1978) 1543.

[15] M.P. Combes *et al.*, Nucl. Phys. **A431** (1984) 703.

[16] D. Ashery *et al.*, Phys. Lett. **B215** (1988) 41; Los Alamos Report LA-UR-88-1023.

[17] N. Willis *et al.*, Phys. Lett. **B229** (1989) 33; M.P. Combes-Comets *et al.*, Phys. Rev. **C43** (1991) 973.

[18] S. Stanislaus *et al.*, Phys. Lett. **B219** (1989) 237.

[19] B. Tatischeff *et al.*, Institut de Physique Nucleaire Orsay, Annual Report 1993, p84.

Table 1. Calculated masses using equations (4) $\rightarrow$ (7), and experimental masses of narrow hadronic structures. ΔM_0 and ΔM_1 are defined by the relation : [(calculated-experimental)/calculated] values between M_0 and M_1 masses.

	M_0 cal.	M_0 exp.	ΔM_0	M_1 cal.	M_1 exp.	ΔM_1
$q - q^2$	851.1	838.2	0.015	100.5	100.3	0.002
q^2 - q^4	1830.4	1841	-0.006	47.6	52.5	-0.10
$q - q^5$	1847.7	1874.6	-0.015	30.3	5.3	0.82
q^2 - $\bar{q}^2$	309.7	310	-0.001	30.3	30	0.01
q^3 - $\bar{q}^3$	310	310	0	30	30	0
q^4 - $\bar{q}^4$	310	357	-0.15	30	27	0.1
$q(q\bar{q})^2$ - q^2	851.1	838.2	0.015	100.5	100.3	0.002